Hybrid catalyst with monoclinic MoTe$_2$ and platinum for efficient hydrogen evolution 🄴🄿

Jinbong Seok 🄵, Jun-Ho Lee 🄵, Dongyeon Bae, Byungdo Ji, Young-Woo Son, Young Hee Lee 🄵, Heejun Yang 🄵, and Suyeon Cho 🄵

COLLECTIONS

🄴🄿 This paper was selected as an Editor's Pick

View Online **Export Citation** **CrossMark**

ARTICLES YOU MAY BE INTERESTED IN

Hybrid catalyst with monoclinic MoTe$_2$ and platinum for efficient hydrogen evolution

View Online   Export Citation   CrossMark

Jinbong Seok,[1,2,a] Jun-Ho Lee,[3,a] Dongyeon Bae,[4] Byungdo Ji,[1] Young-Woo Son,[3] Young Hee Lee,[1,2] Heejun Yang,[1,b] and Suyeon Cho[4,b]

AFFILIATIONS

[1] Department of Energy Science, Sungkyunkwan University, Suwon 16419, South Korea
[2] IBS Center for Integrated Nanostructure Physics (CINAP), Institute for Basic Science, Sungkyunkwan University, Suwon 16419, South Korea
[3] Korea Institute for Advanced Study, Seoul 02455, South Korea
[4] Division of Chemical Engineering and Materials Science, Ewha Womans University, Seoul 03760, South Korea

[a] Contributions: J. Seok and J.-H. Lee contributed equally to this work.
[b] Authors to whom correspondence should be addressed: h.yang@skku.edu and s.cho@ewha.ac.kr

ABSTRACT

Transition metal dichalcogenides (TMDs) are considered as promising catalysts for the hydrogen evolution reaction (HER) owing to their abundant active sites such as atomic vacancies and step edges. Moreover, TMDs have polymorphism, which has stimulated extensive studies on tuning of surface electronic structures for an active HER. The polymorphism in TMDs provides an opportunity for new hybrid catalysts with TMDs and other catalytic metals via surface engineering that can create a novel functional surface of the catalytic electrode for the active HER. Here, we report a hybrid catalyst with monoclinic MoTe$_2$ and platinum (Pt) for the HER. Pt atoms were chemically bound to the surface of monoclinic MoTe$_2$ that has an atomically distorted lattice structure, which produces a distinct Pt-Te alloy layer. The Pt/MoTe$_2$ hybrid catalyst exhibits an active HER with a Tafel slope of 22 mV per decade and an exchange current density of 1.0 mA/cm^2, which are the best values among those reported for TMD-based catalysts. The use of minimum amount of Pt on atomically distorted metallic TMDs realizes rich catalytic active sites on large basal planes for efficient hydrogen production.

Recent progress in two-dimensional energy materials has been highlighted due to their broad applications in photocatalysis, photovoltaics, batteries, supercapacitors, and electrochemical catalysis.[1–6] Electrochemical catalysts based on transition metal dichalcogenides (TMDs) have been intensively studied in hydrodesulfurization, hydrogenation, and the hydrogen evolution reaction (HER).[7–9] In particular, most semiconducting group 6 TMDs such as MoS$_2$, MoSe$_2$, and WS$_2$ have shown excellent electrochemical catalytic performances for the HER at their highly conducting edges or atomic defect sites.[10–12] Despite the active HER performance at certain atomic sites on the surface, the limited surface area of such atomically defined active sites remains an issue, and the industry of hydrogen production requires more efficient and stable electrochemical reactions with reactive sites on the entire surface area. However, the semiconducting basal plane of TMDs without edges or defects has been found to be electrochemically inactive for the HER.[13,14]

Extensive efforts have been made to exploit the whole basal plane of TMDs for the HER by fabricating hybrid catalysts. For example, various catalytic nanoparticles, such as Pt, Pd, and Cu, have been decorated on semiconducting TMD surfaces to make the entire basal planes more active.[15,16] Moreover, in the HER, hybrid TMD catalysts with low dimensional electrodes such as graphene and carbon nanotubes have been suggested as a solution to resolve the high contact resistance between the semiconducting TMDs and metal electrodes.[17–19] The TMD-based catalysts with external nanostructures (nanoparticles, graphene, or carbon nanotubes) or their hybrids have shown improved HER performances than pristine TMDs, but the functional role of the substrate in the simply combined catalyst geometry could not be studied rigorously by density

functional theory calculations, and thus, further improvement of the HER has been limited.

Motivated by the polymorphism of group 6 TMD single crystals, structural phase engineering has also been used to achieve higher HER performances. In the case of MoS$_2$, HER performance is improved when their most stable (hexagonal) semiconducting phase is converted to the metastable (monoclinic or octahedral) metallic phase.[20–22] Experimental and theoretical studies have revealed that effective hydrogen evolution occurs at chalcogen atomic sites on the whole basal plane in the metallic phase, which enhances the total catalytic activity of the TMDs. Nevertheless, the HER performance with metallic TMDs is not high enough for real applications (compared to Pt or other hybrid catalysts), and the metallic phase is metastable, inevitably implying a stability issue in the HER.[23–25]

In contrast to other group 6 TMDs mostly investigated for the HER, MoTe$_2$ possesses two stable structures under ambient conditions: semiconducting hexagonal (2H) and metallic monoclinic (1T$'$) phases that can be selectively synthesized as high quality single crystals.[26] While 2H- and 1T-MoS$_2$ can be controlled by chemical lithium intercalation, the metallic 1T$'$-MoTe$_2$ can be converted from its semiconducting 2H phase via laser-illumination, and strain and Te vacancy creation, making the 1T$'$ phase robust against thermal heating or aging.[27–29] Recently, an atomic-scale study on the HER with the metallic MoTe$_2$ single crystals has been reported by combining DFT calculations and atomic microscopy with the electrochemical measurement.[30,31] The stable metallic 1T$'$-MoTe$_2$, allowing efficient charge transfer at the surface, would be promising for the HER, but the HER performance of 1T$'$-MoTe$_2$ was not on par with that of the conventional Pt catalyst.

In order to fully exploit the whole metallic basal planes as active sites for the HER performance, we propose a Pt/MoTe$_2$ hybrid catalyst where metallic basal planes of MoTe$_2$, having an atomically distorted lattice structure, are coated by Pt atoms via electrochemical activation. The self-structuring of Pt nanoparticles on the carbon-based working electrodes has been observed during electrochemical activation when Pt is used as the counter electrode for the HER.[32–34] The dissolution of Pt atoms in the electrolyte leads to the growth of Pt on the MoTe$_2$ surface by a subsequent reduction process. This idea provides a breakthrough in two aspects: (1) a new chemical state of Pt can be formed on the distorted 1T (1T$'$) MoTe$_2$ surface and (2) the stability can be improved by using a well-defined stable metallic group 6 TMD (1T$'$-MoTe$_2$), compared to that of metastable and inhomogeneous 1T-MoS$_2$. Our Pt/MoTe$_2$ hybrid catalyst shows an excellent HER performance with a Tafel slope of 22 mV per decade and an exchange current density of 1.0 mA/cm^2, which are the best values among those reported for TMD-based catalysts.

We prepared a Pt/MoTe$_2$ hybrid catalyst using the electrochemical method described in Fig. 1(a). The details of experiment are described in the supplementary material. The electrochemical method realized the deposition of a thin Pt layer on the
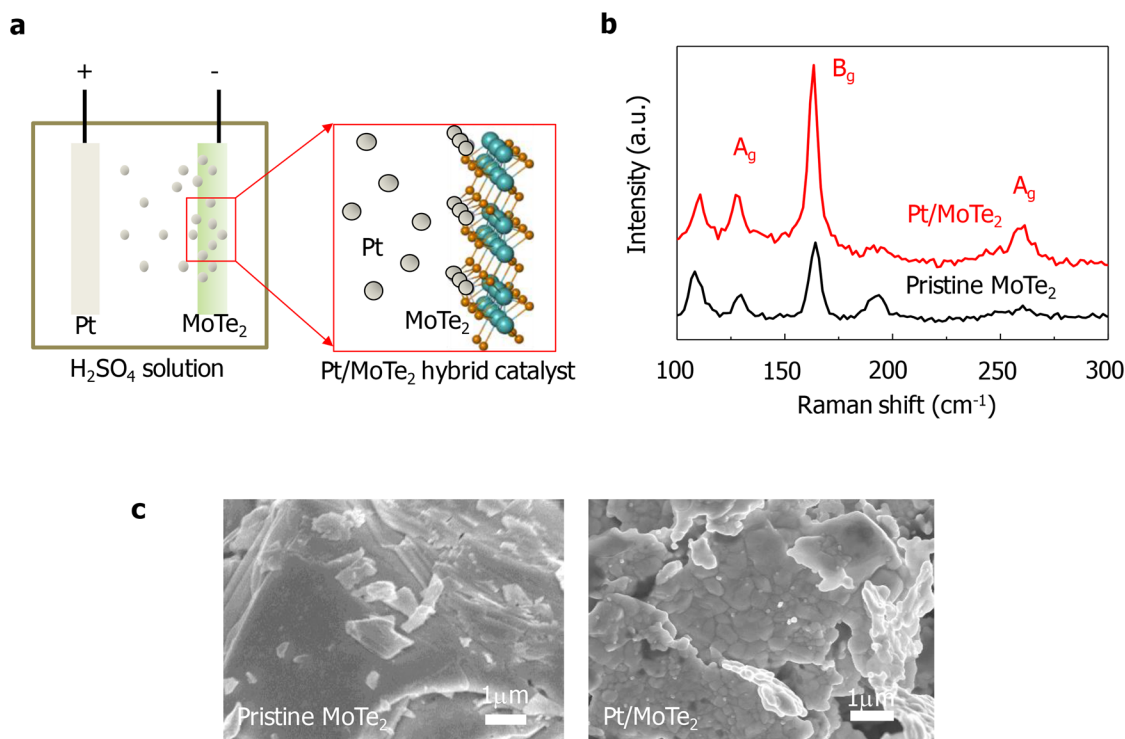

FIG. 1. Preparation of a Pt/MoTe$_2$ hybrid catalyst. (a) Schematic picture of fabricating a Pt/MoTe$_2$ hybrid catalyst via an electrochemical method. (b) Raman spectra of pristine MoTe$_2$ and the Pt/MoTe$_2$ hybrid catalyst. (c) Scanning electron microscope (SEM) images of the pristine MoTe$_2$ single crystal and the Pt/MoTe$_2$ hybrid catalyst.

metallic $MoTe_2$ surface without changing the bulk lattice structures (the structural phase) of the substrate $1T'$-$MoTe_2$. Figure 1(b) supports the identical lattice vibration modes of the $MoTe_2$ by Raman spectra. We used an excitation laser with a power of 2.6 mW and a wavelength of 532 nm for the Raman study, which shows the same Raman modes of A_g and B_g before and after the electrochemical treatment (thin Pt layer deposition) on the monoclinic $MoTe_2$ single crystal. This demonstrates the stability of $1T'$-$MoTe_2$ against additional electrochemical fabrication processes and the suitability as a new metallic TMD substrate for hybrid catalysts. Accordingly, we expected a new chemical state of the thin Pt film on the stable, atomically distorted $1T'$-$MoTe_2$ substrate, which could crucially increase the reactive surface sites for the HER.

Although the bulk crystalline structure of monoclinic $MoTe_2$ was retained in the Pt/$MoTe_2$ hybrid catalyst [Raman spectra in Fig. 1(b)], the morphology of the pristine $MoTe_2$ was modified by the electrochemical deposition of Pt on the $MoTe_2$. The surface change is exhibited in the scanning electron microscope (SEM) images in Fig. 1(c); a clean and flat surface of pristine monoclinic $MoTe_2$ [left picture in Fig. 1(c)] was changed to a corrugated surface with the Pt atoms (right picture) on the $MoTe_2$. We note that, unlike former self-structuring of Pt nanoparticles on TMDs,[16,35] Pt nanoparticles were not observed in the SEM; our electrochemical deposition provided a uniform and well-wetted Pt film on the basal plane of the $MoTe_2$. We explain the formation of the wetted film, rather than nanoparticle formation as previous studies reported, by a unique interaction (a relatively strong bonding) between Pt and distorted chalcogen atoms (Te) in the Pt/$MoTe_2$. More evidence will be

discussed with a chemical state study and corresponding theoretical calculations on the hybrid catalyst.

A progressive improvement of HER performance, as the coverage of the Pt/$MoTe_2$ hybrid increases on the catalyst surface, is described in Fig. 2(a). Starting from the lowest HER performance with pristine monoclinic $MoTe_2$ [orange curve in Fig. 2(a)], the Pt/$MoTe_2$ hybrid catalyst produced higher HER performances, as indicated by the magenta, blue, and red curves in Fig. 2(a). The Tafel slope [22 meV per decade, Fig. 2(b)] and the exchange current density ($\sim$1.0 mA/cm^2) in the red curve [Fig. 2(a)] are better than those of Pt or any other TMD-based catalysts. Other catalytic activities, such as the reversible hydrogen electrode (RHE) potential for a current density of -10 mA/cm^2, the Tafel slope, and the exchange current density of $MoTe_2$, Pt, and Pt/$MoTe_2$ hybrid catalysts are summarized in Table I. The exchange current density was derived from the Tafel curves [Fig. 2(b)] using a linear extrapolation to an overpotential of 0 mV. Figure 2(c) shows that the Pt/$MoTe_2$ hybrid catalyst is more stable than a reference Pt film on SiO_2 under our HER condition over 8000 s. This indicates that the adhesion of Pt on $MoTe_2$ is more stable or stronger than that from the physisorption of Pt on SiO_2; Pt-$MoTe_2$ has chemisorption characteristics or an alloy formation, leading to different surface chemistry from bulk Pt.

To investigate the surface chemical state of the Pt/$MoTe_2$ hybrid catalyst, we conducted X-ray photoemission spectroscopy (XPS) with the pristine $MoTe_2$ [resulting in the orange curve in Fig. 2(a)], the as-prepared Pt/$MoTe_2$ hybrid catalyst [resulting in the red curve in Fig. 2(a)], and the Pt/$MoTe_2$ hybrid catalyst after the stability test [Fig. 2(c)]. Figure 3 shows the core levels of Mo 3d, Te 3d, and Pt 4f electrons by the XPS with fitted lines by Doniac-Sunsic
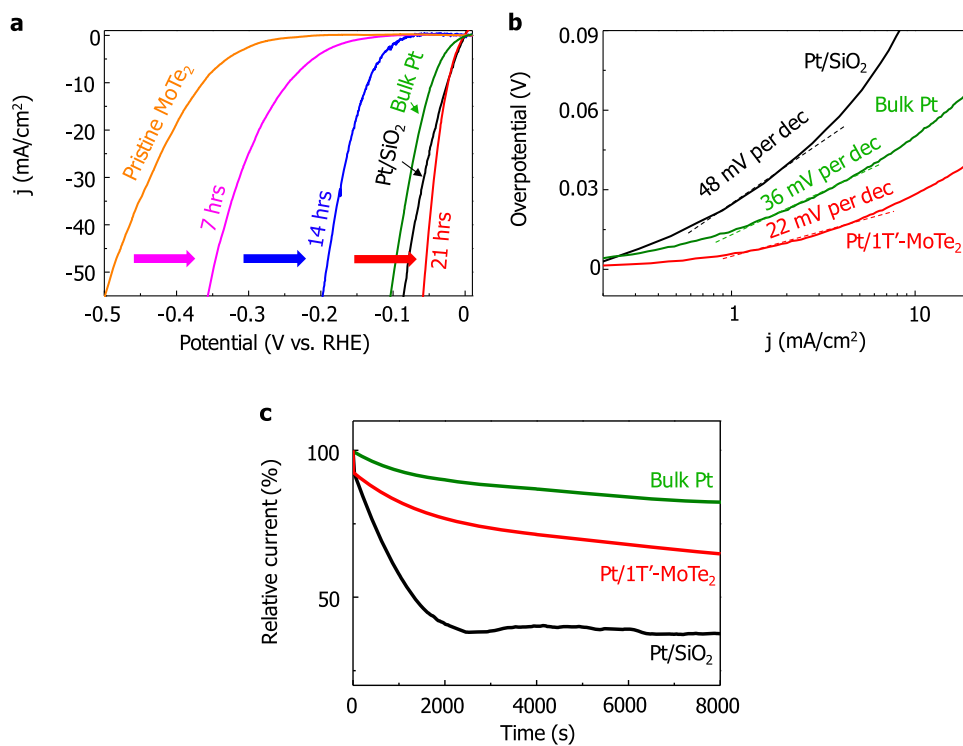
FIG. 2. HER measurements. (a) Polarization curves of bulk Pt rod (green, as a reference), Pt film deposited on SiO_2 (black, as a reference), pristine $MoTe_2$ (orange), and Pt/$MoTe_2$ hybrid catalysts with various treatment times from 7 h to 21 h (magenta, blue, and red). (b) Tafel plots obtained from the polarization curves in Fig. 2(a). (c) A stability comparison between the reference bulk Pt rod (green), Pt thin film deposited on the SiO_2/Si substrate (black), and Pt/$MoTe_2$ hybrid catalyst (red) with a voltage of 0.2 V (vs RHE).

TABLE I. Comparison of catalytic activities.

Catalyst	Potential for −10 mA/cm^2 (V vs RHE)	Tafel slope (mV per decade)	Exchange current density (mA/cm^2)
1T′-MoTe$_2$[30]	−0.356	127	2.1×10^{-2}
Pt/SiO$_2$	−0.024	48	4.5×10^{-1}
Pt/1T′-MoTe$_2$	−0.023	22	1.0

curves. After the electrochemical Pt deposition, Pt 4f and Te 3d photoelectrons were observed as major core levels, indicating that the thickness of the Pt-Te alloy layer is estimated to be ~2 nm, which is the probing depth of the XPS; this enables the minimum amount of Pt with a unique surface chemistry on MoTe$_2$ for an efficient HER. On the as-prepared Pt/MoTe$_2$ hybrid catalyst, the binding energies of Mo 3d and Te 3d electrons [top curves in Fig. 3(a)] are completely different from those of pristine MoTe$_2$ [bottom curves in Fig. 3(a)]. Pt 4f electrons appear in the Pt/MoTe$_2$ [middle curve in Fig. 3(b)], but with chemical states slightly different from the Pt metal [top curve in Fig. 3(b)]. The broadened and asymmetric binding energy features of Pt 4f electrons in the Pt/MoTe$_2$ hybrid catalyst demonstrate the presence of Pt and Pt-Te alloy layers on the surface, which is a key to understand the hybridization of Pt and monoclinic MoTe$_2$.

The deconvolution of the Pt 4f spectrum in Fig. 3(b) clearly shows double peak features (detailed fitting parameters are given in Table II). Considering the reference XPS of the Pt metal [top curve in Fig. 3(b)], the Pt 4f peak located at a binding energy (BE) of 70.74 eV [fitted by a green line in the middle curve in Fig. 3(b)] is assigned to the signal of the pristine Pt metal with a similar Lorentzian width (L.W.) and asymmetry factor (α) by the Doniac-Sunsic fitting (Table II). However, the Pt 4f peak located at 71.72 eV [fitted by a blue line in the middle curve in Fig. 3(b)] could be assigned to a Pt$^{2+\delta}$ signal. Moreover, the Te 3d peak located at 573 eV [fitted by a blue line in Fig. 3(a)] could be assigned to a Te$^{2-\delta}$, demonstrating Pt-Te alloy formation (rather than forming Pt nanoparticles[36]) at the interface between Pt and monoclinic MoTe$_2$. This explains the stability of the Pt-MoTe$_2$ hybrid catalyst in the HER, implying a possible unique surface chemistry of Pt on the top of the catalyst. After the stability
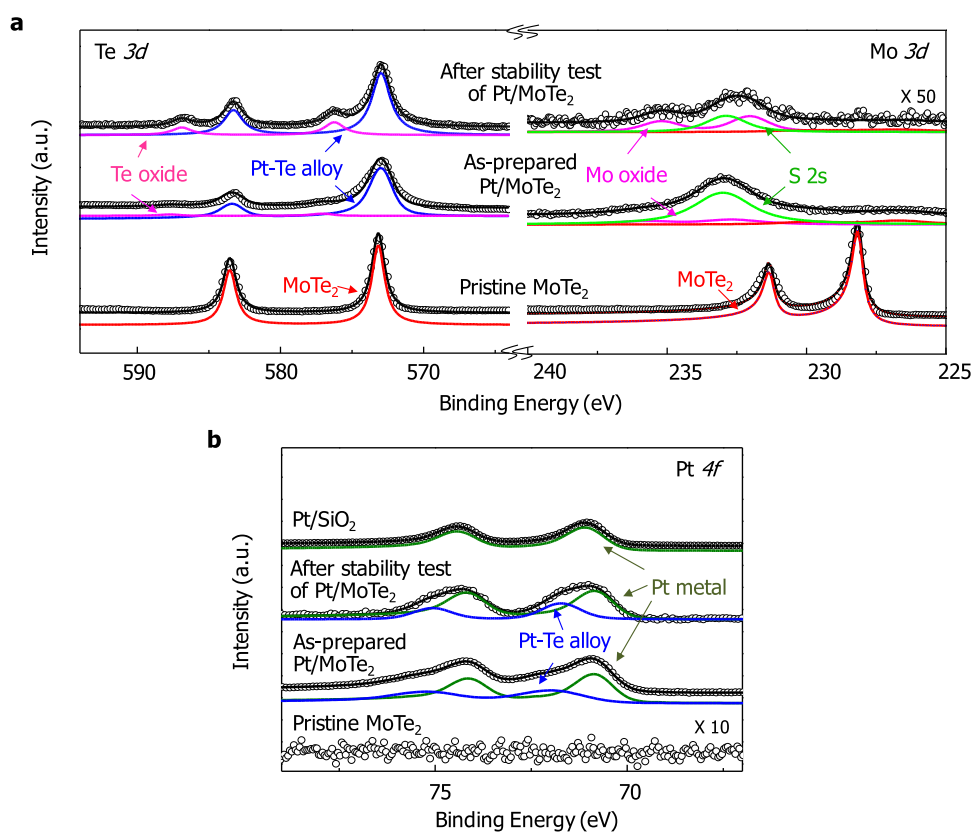

FIG. 3. XPS of pristine MoTe$_2$, as-prepared Pt/MoTe$_2$, and Pt/MoTe$_2$ after the stability test. Core level spectra of (a) Mo 3d and Te 3d electrons, (b) Pt 4f electrons (Pt films on SiO$_2$ were used as a reference to identify the binding energy of Pt 4f in the Pt metal).

TABLE II. Fitting parameters for Pt 4f spectra of Pt/SiO$_2$ and Pt/MoTe$_2$.

	B.E. (eV)	L.W. (eV)	S.O. split (eV)	Asymmetry	Comments
Pt/SiO$_2$	71.19	0.14	3.34	0.19	Metallic Pt
Pt/MoTe$_2$	70.74	0.14	3.34	0.14	Metallic Pt
	71.72	0.35	3.34	0	Pt-Te alloy

test of the Pt-MoTe$_2$ hybrid catalyst, there are small signals from oxide compounds, MoO$_3$ and TeO$_2$ [magenta lines in Fig. 3(a)] with Mo 3d and Te 3d electrons (at 232 eV and 576 eV, respectively) and from absorbed acidic sulfur [light green in Fig. 3(a)] with Mo 3d electrons (at 233 eV), which might arise during the electrochemical process.

To clarify the origin of the high catalytic HER performance of Pt/MoTe$_2$ [Figs. 2(a) and 2(b)], we investigated the Pt adsorption on the top of the MoTe$_2$ surface by first-principles calculations. Since Pt-Te alloys are observed in XPS with a probing depth of ~2 nm (without a pristine Pt signal), we considered the most stable configuration of Pt adsorption at several thicknesses, 0.5 ML, 1.0 ML, 1.5 ML, and 2.0 ML, where 1 ML (monolayer) is defined as two adsorbed Pt atoms in 1 × 1 unit cell of MoTe$_2$ [Fig. 4(a)]. The calculated adsorption energy of the Pt atom on the top of the MoTe$_2$ was found to be large, −4.23 eV, which supports the formation of
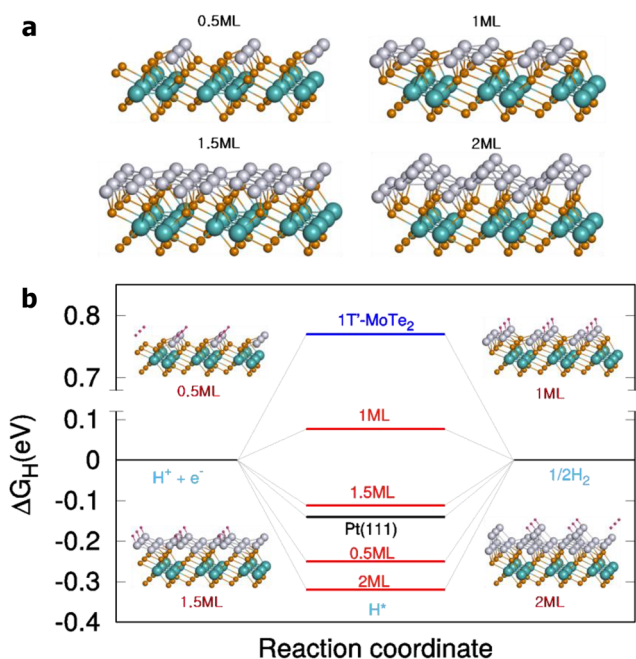

FIG. 4. Schematics of the Pt/MoTe$_2$ hybrid structure at different Pt coverages and ΔG_H of pristine 1T'-MoTe$_2$ and the Pt decorated MoTe$_2$ surface. At a Pt coverage of 1–1.5 ML, the Pt/MoTe$_2$ hybrid catalyst shows an ideal hydrogen adsorption Gibbs free energy change. Green, yellow, gray, and red spheres represent Mo, Te, Pt, and H atoms, respectively.

the Pt-Te alloy rather than Pt nanoparticles as reflected in the XPS measurements (Fig. 3).

Optimizing HER catalysts, a moderate hydrogen adsorption Gibbs free energy change (ΔG_H), close to zero, is critical. In our DFT calculations, the thickness-dependent atomic structure of the Pt/MoTe$_2$ surface results in a significant variation in the ΔG_H. While the ΔG_H on the Pt (111) surface was calculated to be −0.14 eV, the ΔG_H values of the Pt/MoTe$_2$ hybrid catalysts with different Pt thicknesses, 0.5 ML, 1 ML, 1.5 ML, and 2.0 ML, were found to be −0.25 eV, 0.08 eV (±0.22 meV), −0.11 eV (±1.75 meV), and −0.32 eV (±72 meV), respectively.

The calculations of ΔG_H indicate that the buckled geometry of the metallic MoTe$_2$ surface provides a unique surface reconstruction of Pt atoms, which maximizes the catalytic activity and results in excellent HER performances (Fig. 2). Based on the performance of Pt/MoTe$_2$ [red curve in Fig. 2(a)], which is better than that of the reference Pt electrode, we estimate that the coverage (or the thickness) of Pt would be between 1 ML and 1.5 ML. We note that, in contrast to previous TMD-based HER studies that have used unclear active sites, our calculations are convincing given that single-crystalline MoTe$_2$ (and its surface) was adopted for fabricating the hybrid catalyst.

We investigated the catalytic performance of a novel Pt/MoTe$_2$ hybrid catalyst fabricated with a single-crystalline metallic monoclinic MoTe$_2$. The Pt/MoTe$_2$ hybrid catalyst exhibits excellent HER performance, with a Tafel slope of 22 mV per decade and an exchange current density of 1.0 mA/cm^2, which exceeds the HER performance of previous TMD-based catalysts. The highly improved HER originates from rich active sites of the surface of the Pt/MoTe$_2$ hybrid catalyst via a unique reconstruction of Pt atoms on the buckled metallic basal plane. First-principles calculations indicate that H atoms can be adsorbed on the reconstructed Pt/MoTe$_2$ surface with an ideal ΔG_H of 0.08 eV. The strategy of the metallic TMD-based hybridized catalyst has potential for superior catalysis with rich active sites as well as high electric conductivity, which are essential for an active HER with a minimum amount of precious catalytic metals.

See supplementary material for the experimental and calculation schemes.

The authors declare no conflict of interest.

REFERENCES

[1] J. Pang et al., "Applications of 2D MXenes in energy conversion and storage systems," Chem. Soc. Rev. **48**, 72 (2019).

[2] Z. Lin et al., "2D materials advances: From large scale synthesis and controlled heterostructures to improved characterization techniques, defects and applications," 2D Mater. **3**, 042001 (2016).

[3] N. Choudhary et al., "Two-dimensional transition metal dichalcogenide hybrid materials for energy applications," Nano Today **19**, 16 (2018).

[4] J. Pang et al., "Applications of phosphorene and black phosphorus in energy conversion and storage devices," Adv. Energy Mater. **8**, 1702093 (2018).

[5] K. Olszowska et al., "Three-dimensional nanostructured graphene: Synthesis and energy, environmental and biomedical applications," Synth. Met. **234**, 53 (2017).

[6] K. Wang et al., "Synthesis of hydrophobic carbon nanotubes/reduced graphene oxide composite films by flash light irradiation," Front. Chem. Sci. Eng. **12**, 376 (2018).

[7] R. R. Chianelli et al., "Catalytic properties of single layers of transition metal sulfide catalytic materials," Catal. Rev. **48**, 1 (2006).

[8] Y. Qu, H. Pan, and C. T. Kwok, "Hydrogenation-controlled phase transition on two-dimensional transition metal dichalcogenides and their unique physical and catalytic properties," Sci. Rep. **6**, 34186 (2016).

[9] M. Chhowalla et al., "The chemistry of two-dimensional layered transition metal dichalcogenide nanosheets," Nat. Chem. **5**, 263 (2013).

[10] C. Tsai, K. Chan, J. K. Nørskov, and F. Abild-Pedersen, "Theoretical insights into the hydrogen evolution activity of layered transition metal dichalcogenides," Surf. Sci. **640**, 133 (2015).

[11] D. Y. Chung et al., "Edge-exposed MoS_2 nano-assembled structures as efficient electrocatalysts for hydrogen evolution reaction," Nanoscale **6**, 2131 (2014).

[12] R. G. Mendes et al., "Electron-driven in situ transmission electron microscopy of 2D transition metal dichalcogenides and their 2D heterostructures," ACS Nano **13**, 978 (2019).

[13] G. Li et al., "All the catalytic active sites of MoS_2 for hydrogen evolution," J. Am. Chem. Soc. **138**, 16632 (2016).

[14] S. M. Tan et al., "Pristine basal- and edge-plane-oriented molybdenite MoS_2 exhibiting highly anisotropic properties," Chem. - Eur. J. **21**, 7170 (2015).

[15] X. Li et al., "Photo-promoted platinum nanoparticles decorated MoS_2@graphene woven fabric catalyst for efficient hydrogen generation," ACS Appl. Mater. Interfaces **8**, 10866 (2016).

[16] X. Huang et al., "Solution-phase epitaxial growth of noble metal nanostructures on dispersible single-layer molybdenum disulfide nanosheets," Nat. Commun. **4**, 1444 (2013).

[17] S. H. Patil, B. Anothumakkool, S. D. Sathaye, and K. R. Patil, "Architecturally designed Pt–MoS_2 and Pt–graphene composites for electrocatalytic methanol oxidation," Phys. Chem. Chem. Phys. **17**, 26101 (2015).

[18] D. Hou et al., "Pt nanoparticles/MoS_2 nanosheets/carbon fibers as efficient catalyst for the hydrogen evolution reaction," Electrochim. Acta **166**, 26 (2015).

[19] J. Pang et al., "Self-terminating confinement approach for large-area uniform monolayer graphene directly over Si/SiOx by chemical vapor deposition," ACS Nano **11**, 1946 (2017).

[20] A. Ambrosi, Z. Sofer, and M. Pumera, "2H → 1T phase transition and hydrogen evolution activity of MoS_2, $MoSe_2$, WS_2 and WSe_2 strongly depends on the MX_2 composition," Chem. Commun. **51**, 8450 (2015).

[21] D. Voiry et al., "Conducting MoS_2 nanosheets as catalysts for hydrogen evolution reaction," Nano Lett. **13**, 6222 (2013).

[22] J. Wu et al., "Exfoliated 2D transition metal disulfides for enhanced electrocatalysis of oxygen evolution reaction in acidic medium," Adv. Mater. Interfaces **3**, 1500669 (2016).

[23] R. B. Somoano, V. Hadek, and A. Rembaum, "Alkali metal intercalates of molybdenum disulfide," J. Chem. Phys. **58**, 697 (1973).

[24] Q. Tang and D. Jiang, "Mechanism of hydrogen evolution reaction on 1T-MoS_2 from first principles," ACS Catal. **6**, 4953 (2016).

[25] X.-L. Fan et al., "Site-specific catalytic activity in exfoliated MoS_2 single-layer polytypes for hydrogen evolution: Basal plane and edges," J. Mater. Chem. A **2**, 20545 (2014).

[26] D. H. Keum et al., "Bandgap opening in few-layered monoclinic $MoTe_2$," Nat. Phys. **11**, 482 (2015).

[27] S. Cho et al., "Phase patterning for ohmic homojunction contact in $MoTe_2$," Science **349**, 625 (2015).

[28] S. Song et al., "Room temperature semiconductor–metal transition of $MoTe_2$ thin films engineered by strain," Nano Lett. **16**, 188 (2016).

[29] S. Kim et al., "Post-patterning of an electronic homojunction in atomically thin monoclinic $MoTe_2$," 2D Mater. **4**, 024004 (2017).

[30] J. Seok et al., "Active hydrogen evolution through lattice distortion in metallic $MoTe_2$," 2D Mater. **4**, 025061 (2017).

[31] J. C. McGlynn et al., "Molybdenum ditelluride rendered into an efficient and stable electrocatalyst for the hydrogen evolution reaction by polymorphic control," Energy Technol. **6**, 345 (2018).

[32] G. Dong et al., "Insight into the electrochemical activation of carbon-based cathodes for hydrogen evolution reaction," J. Mater. Chem. A **3**, 13080 (2015).

[33] M. Tavakkoli et al., "Electrochemical activation of single-walled carbon nanotubes with pseudo-atomic-scale platinum for the hydrogen evolution reaction," ACS Catal. **7**, 3121 (2017).

[34] L. Zhang et al., "Potential-cycling synthesis of single platinum atoms for efficient hydrogen evolution in neutral media," Angew. Chem. **129**, 13882 (2017).

[35] R. Chen et al., "Use of platinum as the counter electrode to study the activity of nonprecious metal catalysts for the hydrogen evolution reaction," ACS Energy Lett. **2**, 1070 (2017).

[36] B. R. Cuenya et al., "Thermodynamic properties of Pt nanoparticles: Size, shape, support, and adsorbate effects," Phys. Rev. B **84**, 245438 (2011).